

Late Cretaceous palaeomagnetic results from Sikhote Alin, far eastern Russia: tectonic implications for the eastern margin of the Mongolia Block

Yo-ichiro Otofujii,¹ Takaaki Matsuda,^{2*} Ryo Enami,¹ Koji Uno,¹ Katsuhiko Nishihama,¹ Nadir Halim,¹ Li Su,¹ Haider Zaman,¹ Ruslan G. Kulinich,³ Petr S. Zimin,³ Anatoly P. Matunin⁴ and Vladimir G. Sakhno⁴

¹Department of Earth and Planetary Sciences, Faculty of Science, Kobe University, Kobe, Japan. E-mail: otofujii@kobe-u.ac.jp

²Department of Geology, Faculty of Science, Himeji Institute of Technology, Himeji, Japan

³Russian Academy of Science, Pacific Oceanological Institute, Vladivostok, Russia

⁴Russian Academy of Science, Far East Geological Institute, Vladivostok, Russia

Accepted 2002 July 28. Received 2002 May 2; in original form 2001 April 23

SUMMARY

We present palaeomagnetic results from Late Cretaceous welded tuffs in the Kisin Group (Monastirskaya Suite, Primorskaya Series) collected at 27 sites from the Sikhote Alin mountain range. A high unblocking temperature magnetization component ($>590^{\circ}\text{C}$) was isolated after stepwise thermal demagnetization from 25 sites. Combined with previously reported data, reliable characteristic remanence directions from 39 sites are distributed at eight areas ranging from 46.7°N , 138.1°E to 43.4°N , 134.8°E in the Sikhote Alin Block. The bedding-tilt test is positive for two area mean directions and inconclusive for the remaining six areas. The data set for all 39 sites reveals a positive bedding-tilt test at the 99 per cent confidence level, and their tilt-corrected mean direction is $D = 335.6^{\circ}$, $I = 54.4^{\circ}$ ($\alpha_{95} = 8.5^{\circ}$), corresponding to a palaeopole at 71.5°N , 38.9°E with $A_{95} = 9.9^{\circ}$. This westerly direction is ascertained through the tilt-corrected mean direction ($D = 331.1^{\circ}$, $I = 53.5^{\circ}$, $\alpha_{95} = 8.5^{\circ}$) based on the 25 data selected from four areas (Kema river, Terney, Plastun and Moryak-Rybolov) where each data set passes the positive bedding-tilt test or reveals an increase in the precision parameter after tilt correction. Palaeomagnetic declination indicates that the Sikhote Alin Block has rotated counterclockwise by $41^{\circ} \pm 16^{\circ}$ with respect to the Eurasian continent between Late Cretaceous times and 53–50 Ma. Compared with palaeomagnetic data from the surrounding regions, we find that the rotation recorded in Sikhote Alin extends westward into the interior of the Mongolia Block. The eastern margin of the Asian continent experienced both counterclockwise rotation of the eastern part of the Mongolia Block and clockwise rotation of the eastern part of the North China Block over the Cretaceous. We interpret these data in terms of a strong net horizontal force towards the ocean side, acting on the lithosphere at the eastern margin of the Asian continent between the Late Cretaceous and 53–50 Ma. Intermittently occurring upwellings of mantle and associated horizontal flows may have played an important role in producing the net horizontal force acting on the continental block during Late Cretaceous times.

Key words: continent, deformation, Mongolia Block, Palaeomagnetism, Sikhote Alin, tectonics.

1 INTRODUCTION

Palaeomagnetic studies of continental margins offer important clues to the deformation of the continental lithosphere. The large-scale

deformation of entire continents can be detected from a comparison of palaeomagnetic directions from either margin and regional deformation is inferred from the difference in contemporary palaeomagnetic directions by comparison of the continental margin and the interior of the continent.

Deformation along the eastern margin of the Asian continent has been discovered and described by palaeomagnetists over the

*Deceased September 12, 2001.

previous two decades. The Japanese and Ryukyu island arcs appear to have rifted from the Asian continent in association with the opening of the Japan Sea and Okinawa Trough (Otofujii *et al.* 1985; Miki 1995). The many blocks comprising Sakhalin experienced a domino style deformation during the subduction of the Pacific Plate (Takeuchi *et al.* 1999). The Korean peninsula and environs have been subjected to clockwise rotational motion with respect to the interior of the Asian continent since the Cretaceous (Ma *et al.* 1993; Zhao *et al.* 1999; Uno 2000). A large northward movement of the eastern part of Asia is implied by palaeomagnetic data from Korea and Japan (Lee *et al.* 1987; Otofujii 1996). In addition to these regional deformational phenomena, deformation of the whole Asian continent during Cenozoic times is inferred from a comparison of palaeomagnetic directions from eastern and western parts of the Eurasian continent and from its central part (Cogné *et al.* 1999).

The Sikhote Alin mountain area is located at the easternmost part of the Mongolia Block in the Eurasian continental margin bordering the northern Japan Sea (Fig. 1). Before the Japanese islands rifted from the Asian continent in the Early Miocene, the Sikhote Alin was

an extreme margin of the Asian continent bounded by oceanic plates. The Sikhote Alin area is therefore suitable for studying deformation of the Mongolia Block prior to opening of the Japan Sea. In this study we present palaeomagnetic results from Late Cretaceous welded tuffs from the Sikhote Alin area. We have extended our study from areas previously covered by Uno *et al.* (1999) up to 46.38°N latitude in order to understand the tectonics of the main part of the Sikhote Alin after Late Cretaceous times and provide more reliable data than those published in previous work on lavas from this region (Bretstein 1988).

2 GEOLOGICAL SETTING AND SAMPLING

The Mongolia Block constitutes the eastern part of the Asian continent, together with the Siberia Block, North China Block (NCB) and South China Block (SCB). It is bounded to the north by the Mongol–Okhotsk Suture and to the south by the Suolun–Xilamulun suture. A distribution of mountain ranges and basins characterizes

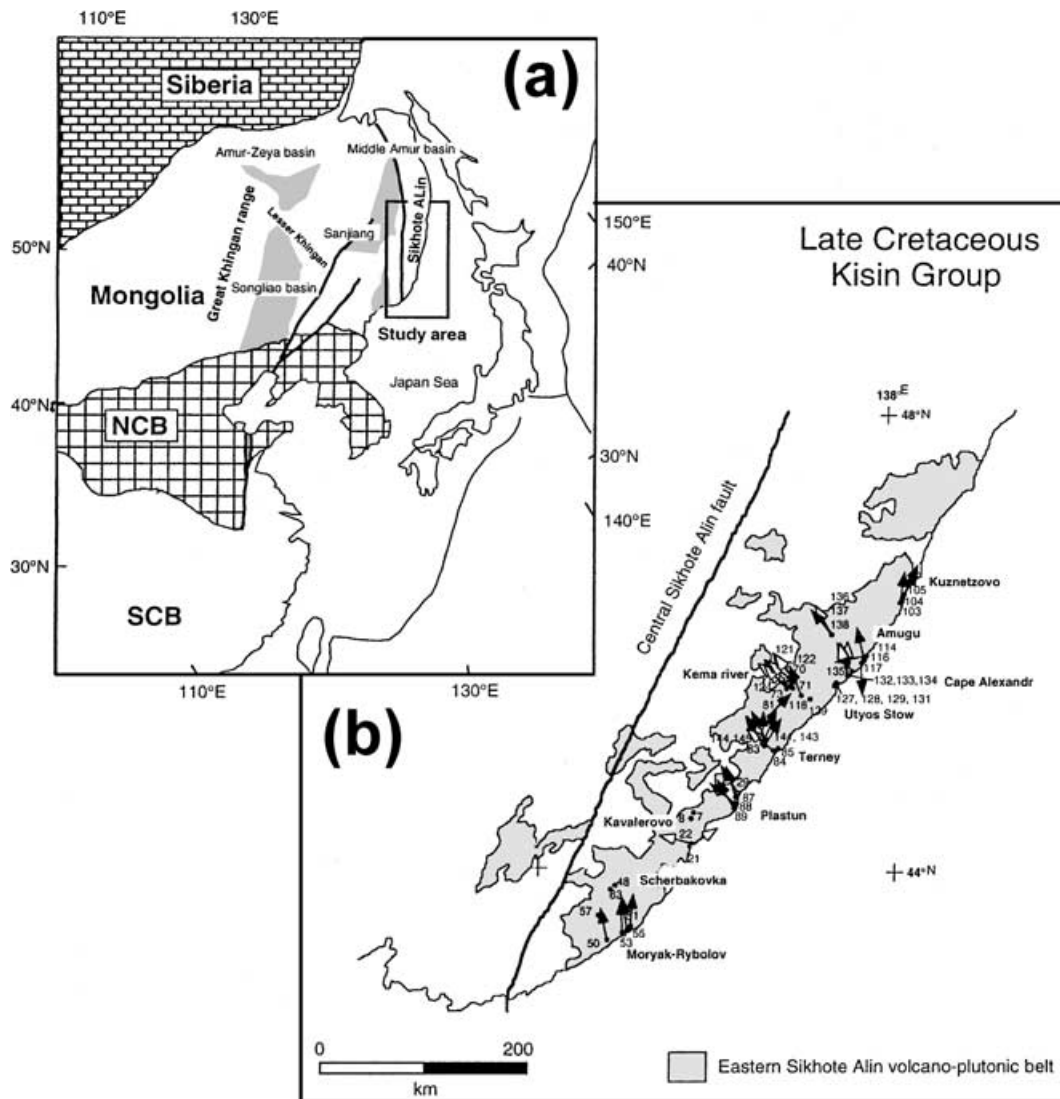


Figure 1. (a) Sketch map of the study area and (b) a map showing the sampling localities of the Kisin Group in Sikhote Alin. (a) Shaded areas show the Cretaceous to Cenozoic basins and grabens. (b) Arrows indicate the mean palaeomagnetic declination at sampling sites. Solid arrows mark directions with normal polarity and open arrows mark directions with reversed polarity. Shaded area indicates the distribution of Late Cretaceous to Palaeocene welded tuffs.

topography of the eastern part of the Mongolia Block: from west to east, we can distinguish the Great Khingan range, the Amur-Zeya and the Songliao basins, the Lesser Khingan range, the Amur basin–Sanjiang basin–the Razdolnians rifts and the Sikhote Alin mountain range (Fig. 1).

The Sikhote Alin volcanic belt covers an area 100 km in width and 1000 km length near the Sikhote Alin mountain range along the Japan Sea coast. It was formed by extensive volcanic activity accompanied by emplacement of plutons from 80 to 50 Ma at the eastern flank of the Precambrian Khingan-Bureya and Khankai massifs (Zonenshain *et al.* 1990; Natal' in 1993; Faure *et al.* 1995; Golozubov & Khanchuk 1996). Middle–Late Jurassic accretionary prisms and diverse Early Cretaceous terranes, form the basement of the Sikhote Alin belt, and are cut by a left-lateral strike-slip fault system. Movements on these faults were either coeval with, or slightly earlier than, the Late Cretaceous volcanic activity (Zonenshain *et al.* 1990).

Volcanic rocks of the Sikhote Alin belt are mostly acid to intermediate welded pyroclastics with interleaved lavas and clastic rocks. Rhyolitic welded tuffs of the Kisin Group (Monastirskaya Suite, Primorskaya Series) are the earliest ignimbrites in the volcanic sequence and form voluminous and extensive shields in Sikhote Alin (Matyunin 1988; Sakhno *et al.* 1991). This group is assigned a Late Campanian age from subtropical Monastyrsky horizon flora (Krassilov 1990). Subsequent volcanism was associated with large caldera formation, and produced andesitic to rhyolitic welded tuffs of the Sijanov Group (66–52 Ma) and rhyolitic welded tuffs of the Bogopol Group (53–50 Ma) studied by Otofujii *et al.* (1995) and Matsuda *et al.* (1998).

Palaeomagnetic samples were collected at 27 sites in six areas (Kuznetsovo, Amugu, Cape Alexander, Utyos Stow, Kema river and Terney) from welded tuffs of the Kisin Group between 1994 and 1997 (Fig. 1). Ten or 11 hand samples, oriented by a magnetic compass, were distributed over distances ranging up to 20 m at each site. Accurate positioning of sites was determined by a portable navigational instrument (Sony PYXIS). Bedding planes were observed in all the sampling sites on the basis of eutaxitic structure (lineation of stretched pumice and aligned phenocrysts). The present geomagnetic field declination value at each sampling site was evaluated from the International Geomagnetic Reference Field (IAGA Division V, 1995).

3 PALAEOMAGNETISM

Individual specimens 25 mm in diameter and 22 mm long were prepared from samples in the laboratory. Natural remanent magnetizations (NRM) were measured with either a spinner magnetometer (Natsuhara SMM-85) or a cryogenic magnetometer (ScT and 2G) depending on the intensity of magnetization. Specimens were thermally demagnetized using a laboratory-built furnace with a residual magnetic field lower than 10 nT during the cooling cycle. Results for each specimen were plotted on orthogonal vector diagrams (Zijderveld 1967) to assess component structures, and on equal-area projections to evaluate directional stability. Principal-component analysis (Kirschvink 1980) was used to estimate the component directions. Palaeomagnetic results are listed in Table 1.

3.1 Demagnetization

The NRM intensity of the 27 sites ranges between $3.0 \times 10^{-3} \text{ A m}^{-1}$ (SA121) and 5.5 A m^{-1} (SA137). Similar demagnetization behaviour is observed in specimens from each site except two (SA137 and SA139). Single-component magnetization is observed at one

site (Fig. 2e), two-component magnetization at 21 sites (Figs 2a–d) and three-component magnetization at three sites (Fig. 2f). The single-component and the highest-temperature component in the multicomponent magnetizations reveal straightforward decay with unblocking temperatures between of 560 and 650 °C, indicating that the component resides in both magnetite and haematite. The lowest-temperature component in the multicomponent magnetization is erased at temperatures of between 250 and 560 °C. Since the *in situ* direction is subparallel to the geocentric axial dipole field, the low-temperature component is probably a viscous or viscous partial thermoremanent magnetization, acquired in the recent geomagnetic field (Pullaiah *et al.* 1975).

Specimens of SA137 (4.7×10^{-3} – $5.5 \times 10^0 \text{ A m}^{-1}$) from Amugu and SA139 (3.8×10^{-2} – $8.1 \times 10^{-1} \text{ A m}^{-1}$) from Kema river have variable remanent magnetization intensities, and variable demagnetization behaviours within each site display up to three-component magnetizations. Remanent directions of the highest-temperature component illustrate clockwise curl in each site. Because these two sites are located on the top of a mountain, their remanent magnetizations are probably IRMs caused by lightning strikes and they are omitted from further discussion.

We re-examined demagnetization behaviour of specimens from six sites (SA07, SA08, SA48, SA57, SA63 and SA85) from the Terney, Kavalerova and Scherbakovka areas in the southern part of Sikhote Alin (Fig. 3), because Uno *et al.* (1999) suggest that these sites acquired secondary remanent magnetization during subsequent igneous activity. Four-component magnetization is observed in specimens at SA57 and SA63. An abrupt decrease of remanent intensity between 300 and 350 °C in specimens of SA85 is indicative of the presence of pyrrhotite or maghemite, which are probably connected with ore deposition processes in Sikhote Alin regions. Because welded tuffs in these rocks seem to have been subjected to a secondary magnetization process, we reject data from the above six sites for the same reasons as Uno *et al.* (1999).

3.2 Palaeomagnetic directions

Combining with palaeomagnetic directions reported previously (Uno *et al.* 1999), the total number of sampling sites in the Kisin group is increased to 43. The 43 sites are from nine areas extending from 43.36°N (SA50) to 46.38°N (SA105) (Fig. 1). The high-temperature component directions are clustered tightly in each site and precision parameters (*k*) of site mean directions range from 21.0 to 902.7. The 95 per cent confidence circles do not exceed 13°. Site mean directions are listed before and after tilt correction in Table 1.

The Utyos Stow area records geomagnetic field reversal in sequentially stratified layers at four sites (Table 1). An easterly direction with shallow positive inclination (SA129) follows the northeasterly direction with positive inclination of the lowest layers (SA127, SA128). A westerly direction with negative inclination appears in the uppermost layer (SA131).

Site mean palaeomagnetic directions of 39 sites (before and after tilt correction) from the remaining eight areas are shown in Fig. 4. 24 sites have normal polarity and 15 have reversed polarity. An exclusively normal (Kuznetsovo, Plastun and Moryak-Rybolov areas) or reversed (Kavalerovo) polarity is observed in four areas, whereas the remaining four areas (Amugu, Cape Alexander, Kema river and Terney areas) revealed mixed polarities. The counterclockwise deflected directions from the north or south are predominant throughout the studied area.

Table 1. Summary of paleomagnetic results of the Late Cretaceous Kisin Group (Rhyolite welded tuffs)

| Locality | Site Name | Latitude | Longitude | N | In-situ | | Tilt-corrected | | k | a95 (.) | strike (.) | Dip (.) | |
|--|-----------|----------|-----------|--------|---------|-------|----------------|-------|-------|------------|---------------|------------|----|
| | | | | | D(.) | I(.) | D(.) | I(.) | | | | | |
| Kuznetsovo | SA105 | 46.38 | 138.14 | 10 | 33.1 | 54.7 | 21.6 | 75.1 | 222.7 | 3.2 | 132 | 21 | |
| | SA104 | 46.37 | 138.13 | 10 | 31.1 | 10.8 | 27.8 | 4.4 | 152.8 | 3.9 | 224 | 25 | |
| | SA103 | 46.37 | 138.13 | 10 | 7.0 | 32.4 | 8.3 | 25.8 | 213.8 | 3.3 | 297 | 7 | |
| | mean | 44.00 | 135.00 | 3 | 21.3 | 28.6 | | | 9.5 | 42.4 | | | |
| | | | | | | | 17.0 | 30.4 | 4.4 | 68.1 | | | |
| Amugu | SA137 | | | | | | | | | | 297 | 28 | |
| | SA136 | 46.02 | 137.30 | 10 | 151.5 | -51.8 | 151.0 | -56.8 | 43.4 | 7.4 | 65 | 5 | |
| | SA138 | 46.01 | 137.29 | 10 | 325.4 | 27.3 | 322.4 | 1.6 | 187.3 | 3.5 | 210 | 28 | |
| | SA114 | 45.83 | 137.69 | 11 | 294.5 | 53.9 | 274.7 | 77.7 | 329.0 | 2.5 | 35 | 25 | |
| | SA116 | 45.82 | 137.69 | 10 | 357.7 | 67.0 | 354.8 | 80.0 | 210.0 | 3.3 | 90 | 13 | |
| | SA117 | 45.82 | 137.69 | 10 | 276.5 | 73.4 | 177.9 | 66.8 | 191.6 | 3.5 | 55 | 31 | |
| | mean | 44.00 | 135.00 | 5 | 320.4 | 56.8 | | | 12.1 | 22.9 | | | |
| | | | | | | 316.3 | 67.6 | 4.1 | 43.0 | | | | |
| Cape Alexandr | SA135 | 45.70 | 137.52 | 10 | 309.0 | 56.0 | 332.5 | 60.3 | 117.1 | 4.5 | 337 | 15 | |
| | SA132 | 45.67 | 137.49 | 10 | 148.9 | -54.5 | 166.0 | -37.8 | 56.1 | 6.5 | 292 | 23 | |
| | SA133 | 45.67 | 137.49 | 10 | 152.4 | -52.0 | 173.2 | -33.9 | 150.9 | 3.9 | 304 | 28 | |
| | SA134 | 45.67 | 137.49 | 10 | 157.5 | -52.6 | 165.5 | -35.4 | 348.6 | 2.6 | 277 | 19 | |
| mean | 44.00 | 135.00 | 4 | 327.3 | 53.8 | | | 115.5 | 8.6 | | | | |
| | | | | | | 344.8 | 40.4 | 32.9 | 16.3 | | | | |
| Utyos Stow | SA131 | 45.60 | 137.35 | 10 | 262.3 | -66.2 | 259.5 | -31.3 | 23.6 | 10.2 | 347 | 35 | |
| | SA129 | 45.59 | 137.34 | 9 | 95.1 | 19.5 | 93.0 | 11.6 | 124.1 | 4.6 | 320 | 11 | |
| | SA128 | 45.58 | 137.33 | 8 | 39.8 | 61.5 | 47.6 | 37.3 | 21.0 | 12.4 | 329 | 25 | |
| | SA127 | 45.58 | 137.33 | 10 | 41.4 | 60.8 | 27.4 | 47.0 | 116.6 | 4.5 | 268 | 17 | |
| Kema river | SA121 | 45.63 | 136.85 | 10 | 123.4 | -53.3 | 142.4 | -7.9 | 177.3 | 3.6 | 257 | 53 | |
| | SA124 | 45.63 | 136.84 | 10 | 121.1 | -47.4 | 125.5 | -44.8 | 312.7 | 2.7 | 272 | 5 | |
| | SA72* | 45.63 | 136.81 | 10 | 118.6 | -49.1 | 127.4 | -39.7 | 902.7 | 1.6 | 257 | 13 | |
| | SA73* | 45.63 | 136.81 | 10 | 126.9 | -36.7 | 136.3 | -26.6 | 55.0 | 6.6 | 278 | 18 | |
| | SA122 | 45.62 | 136.86 | 10 | 105.6 | -53.9 | 143.5 | -41.2 | 221.5 | 3.3 | 285 | 35 | |
| | SA123 | 45.62 | 136.86 | 10 | 118.5 | -54.9 | 124.3 | -60.9 | 452.7 | 2.3 | 0 | 7 | |
| | SA70* | 45.62 | 136.82 | 10 | 117.5 | -40.8 | 121.5 | -34.7 | 677.0 | 1.9 | 250 | 8 | |
| | SA71* | 45.62 | 136.84 | 10 | 127.0 | -42.7 | 123.0 | -40.6 | 487.3 | 2.2 | 150 | 5 | |
| | SA118 | 45.49 | 136.98 | 9 | 19.4 | 63.9 | 339.3 | 67.0 | 115.7 | 4.8 | 170 | 18 | |
| | SA139 | | | | | | | | | | 78 | 20 | |
| | mean | 44.00 | 135.00 | 9 | 304.8 | 51.3 | | | 24.7 | 10.6 | | | |
| | | | | | | | 312.5 | 40.8 | 17.6 | 12.6 | | | |
| | Terney | SA81* | 45.31 | 136.57 | 10 | 52.0 | 56.9 | 44.0 | 63.5 | 122.1 | 4.4 | 173 | 8 |
| | | SA82* | 45.11 | 136.53 | 8 | 26.4 | 42.6 | 21.0 | 64.3 | 450.6 | 2.6 | 124 | 22 |
| SA83* | | 45.10 | 136.53 | 7 | 31.1 | 50.5 | 31.1 | 50.5 | 63.5 | 7.6 | 0 | 0 | |
| SA141 | | 45.10 | 136.52 | 11 | 13.1 | 50.4 | 332.7 | 64.6 | 162.0 | 3.6 | 145 | 28 | |
| SA143 | | 45.08 | 136.47 | 10 | 308.8 | 16.5 | 328.0 | 43.7 | 23.0 | 10.3 | 358 | 41 | |
| SA144 | | 45.08 | 136.47 | 7 | 315.8 | 9.0 | 329.4 | 33.0 | 25.7 | 12.1 | 357 | 41 | |
| SA145 | | 45.08 | 136.47 | 10 | 319.7 | 25.1 | 0.5 | 65.4 | 40.5 | 7.7 | 25 | 52 | |
| SA84* | | 45.03 | 136.64 | 9 | 119.0 | -39.2 | 130.6 | -72.6 | 378.6 | 2.6 | 22 | 34 | |
| SA85* | | 45.03 | 136.64 | 8 | 170.6 | -58.1 | 224.3 | -60.7 | 190.1 | 4.0 | 22 | 30 | |
| mean | | 44.00 | 135.00 | 8 | 342.1 | 42.9 | | | 5.0 | 27.7 | | | |
| | | | | | | | 353.3 | 60.3 | 13.8 | 15.5 | | | |
| Plastun | SA29* | 44.63 | 136.20 | 10 | 328.2 | 61.3 | 329.4 | 49.4 | 382.4 | 2.5 | 243 | 12 | |
| | SA87* | 44.61 | 136.22 | 10 | 319.0 | 62.1 | 343.0 | 48.5 | 550.1 | 1.9 | 292 | 21 | |
| | SA88* | 44.60 | 136.22 | 9 | 300.1 | 35.1 | 308.7 | 63.3 | 56.5 | 6.9 | 20 | 29 | |
| | SA89* | 44.60 | 136.22 | 9 | 309.5 | 34.7 | 330.0 | 45.2 | 385.6 | 2.6 | 343 | 26 | |
| | mean | 44.00 | 135.00 | 4 | 311.5 | 49.1 | | | 22.6 | 19.8 | | | |
| | | | | | | 329.4 | 52.0 | 50.5 | 13.1 | | | | |
| Kavalerova | SA07* | 44.47 | 135.70 | 9 | 185.4 | -65.1 | 238.5 | -84.5 | 101.5 | 5.1 | 83 | 22 | |
| | SA08* | 44.47 | 135.70 | 6 | 183.3 | -59.4 | 169.7 | -61.5 | 127.9 | 5.9 | 80 | 15 | |
| | SA22* | 44.16 | 135.65 | 10 | 26.5 | -84.9 | 104.1 | -61.4 | 124.0 | 4.4 | 205 | 28 | |
| | SA21* | 44.15 | 135.63 | 10 | 322.6 | -79.1 | 235.7 | -88.2 | 120.0 | 4.4 | 242 | 11 | |
| | mean | 44.00 | 135.00 | 2 | 159.4 | 83.0 | | | *** | *** | | | |
| | | | | | | 287.2 | 76.6 | *** | *** | | | | |
| Scherbakovka | SA48* | 43.81 | 134.83 | 9 | 194.0 | -67.8 | 149.0 | -57.8 | 27.7 | 10.0 | 194 | 24 | |
| | SA63* | 43.79 | 134.78 | 10 | 202.1 | -52.1 | 197.0 | -53.0 | 516.0 | 2.1 | 187 | 4 | |
| | SA57* | 43.57 | 134.66 | 7 | 185.8 | -64.3 | 199.8 | -37.3 | 215.2 | 4.1 | 305 | 29 | |
| | mean | 44.00 | 135.00 | 3 | 15.1 | 61.8 | | | 78.7 | 14.0 | | | |
| | | | | | | 5.5 | 51.9 | 16.3 | 31.6 | | | | |
| Moryak-Rybolov | SA51* | 43.47 | 134.97 | 8 | 58.6 | 66.4 | 5.0 | 69.3 | 45.9 | 8.3 | 205 | 21 | |
| | SA55* | 43.46 | 134.96 | 10 | 46.8 | 73.1 | 352.1 | 62.7 | 88.1 | 5.2 | 223 | 23 | |
| | SA53* | 43.45 | 134.94 | 10 | 16.6 | 85.2 | 358.2 | 71.5 | 116.7 | 4.5 | 262 | 14 | |
| | SA50* | 43.36 | 134.78 | 10 | 336.9 | 54.6 | 348.5 | 36.7 | 362.1 | 2.5 | 285 | 21 | |
| | mean | 44.00 | 135.00 | 4 | 19.3 | 74.0 | | | 19.0 | 21.7 | | | |
| | | | | | | 354.0 | 60.8 | 25.5 | 18.6 | | | | |
| Mean (whole sites) | before | 44.00 | 135.00 | 39 | 330.1 | 56.2 | | | 7.6 | 8.9 | | | |
| | after | 44.00 | 135.00 | 39 | | | 335.6 | 54.4 | 8.3 | 8.5 | | | |
| | | | | | | | | | | | VGP | | |
| | | | | | | | | | | | Lat. | A95 | |
| | | | | | | | | | | | 71.5°N | 9.9°E | |
| Mean (selected sites; Kema river, Terney, Plastun, Moryak-Rybolov) | before | 44.00 | 135.00 | 25 | 324.2 | 54.4 | | | 7.9 | 11.0 | | | |
| | after | 44.00 | 135.00 | 25 | | | 331.1 | 53.5 | 12.7 | 8.5 | | | |

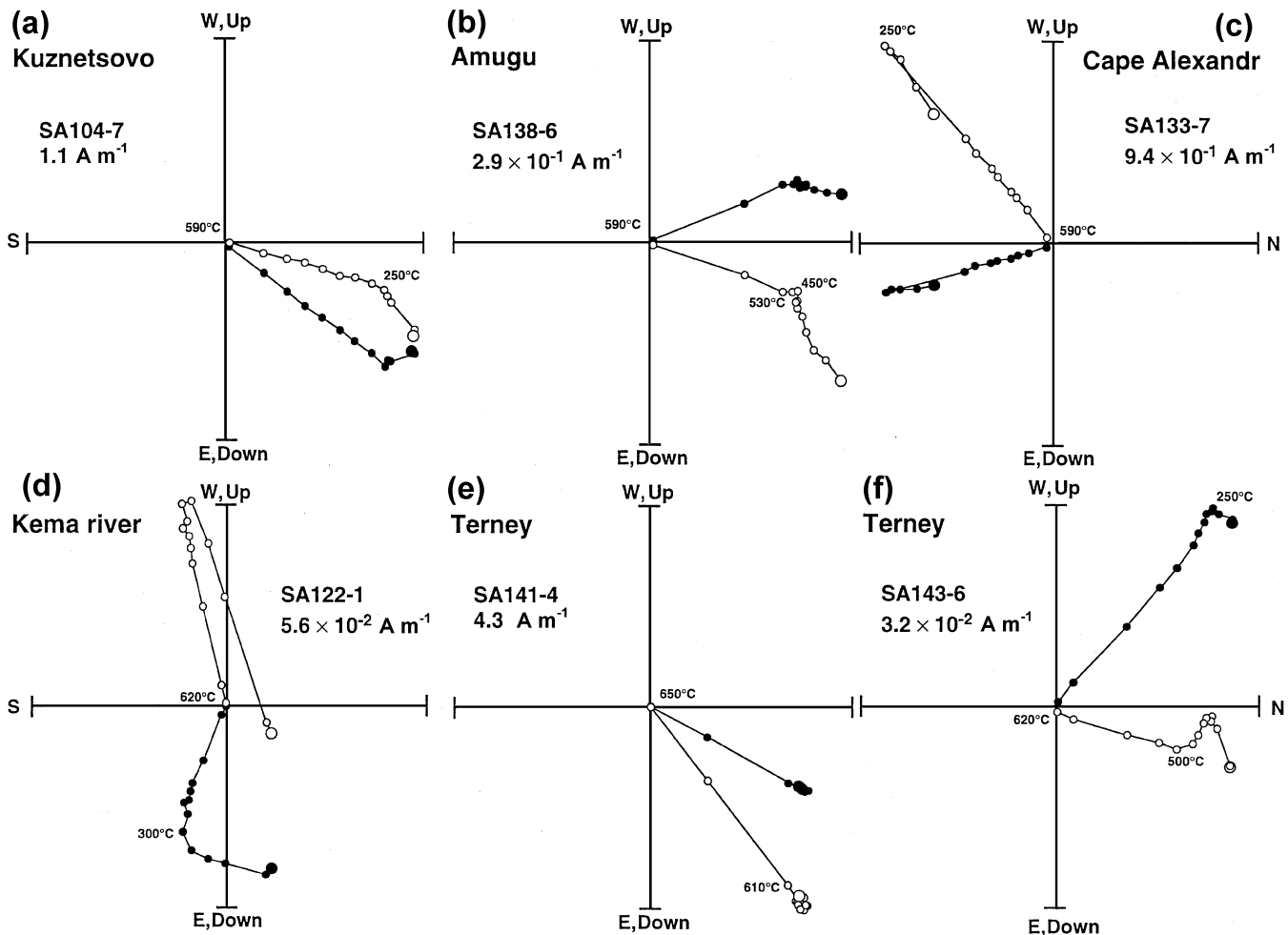


Figure 2. Orthogonal projections of magnetization vector end points during thermal demagnetization experiments for five areas of the Kisin Group. (a–d) Examples with two-component magnetization, (e) an example with single component magnetization and (f) an example of three-component magnetization. Open symbols show the magnetization vector projection on to the vertical plane, solid symbols on to the horizontal plane. Directions are *in situ*.

In contrast to normal polarity sites, the southeasterly reversed polarity directions from 15 sites show an increase in scattering after bedding-tilt correction. This type of behaviour may be caused by a difference in distribution of the normal and reversed polarity sampling areas. Sampling sites with normal polarities are distributed throughout the area studied, whereas the reversed polarity sites are restricted to some localized zones. 11 out of 15 sites are collected from two localized areas, i.e. the Cape Alexander and the Kema river areas. Since sampling sites at Cape Alexander (SA132, SA133 and SA134) covered a very small area with almost the same bedding attitude, an identical palaeomagnetic direction is in agreement with expectations. Although a small dispersion is evident after tilt correction, the *in situ* directions for these sites are clustered around $D/I = 150^\circ/-52^\circ$. Eight sampling sites collected along the Kema river are distributed within the 5.5 km area in order from up- to downstream as SA72, SA73, SA70, SA71, SA124, SA121, SA123 and SA122. These eight palaeomagnetic directions form a cluster around $D/I = 120^\circ/-50^\circ$ in geographic coordinates, but show a remarkable dispersion with split groupings after tilt correction. Although, the dispersion of tilt-corrected directions from Cape Alexander and Kema river areas may create an idea of remagnetization; however, according to our opinion the behaviour can probably be caused by some uncertainties in reading the correct bedding attitude of the welded

tuffs. The dispersions of untilted reversed polarity directions can also be attributed to a small sampled area where no significant change in bedding attitude is observed. In order to obtain an idealized tilt correction of the target area more widely distributed sampling sites with clear and variable bedding attitude should be the focus of any future field trip.

3.3 Analysis of results

At first, we calculated the area palaeomagnetic mean directions for the eight areas. The clustering of directions on structural correction improves in the Terney, Plastun and Moryak-Rybolov areas, whereas other areas reveal scattering. The bedding-tilt test of McFadden (1990) was applied to the area mean directions. The Kema river and Terney areas pass the bedding-tilt test at the 99 per cent confidence level, and the tests for the remaining six areas are not negative but are inconclusive. Because the bedding-tilt test is not negative for each area mean, no data sets for any areas are discarded because of post-tilting magnetizations. A two-component magnetization characterizes demagnetization behaviour for specimens with reversed directions and counterclockwise deflection in declination is observed in specimens with normal directions. Recent study indicates that the reversed direction of the Bogopol Group

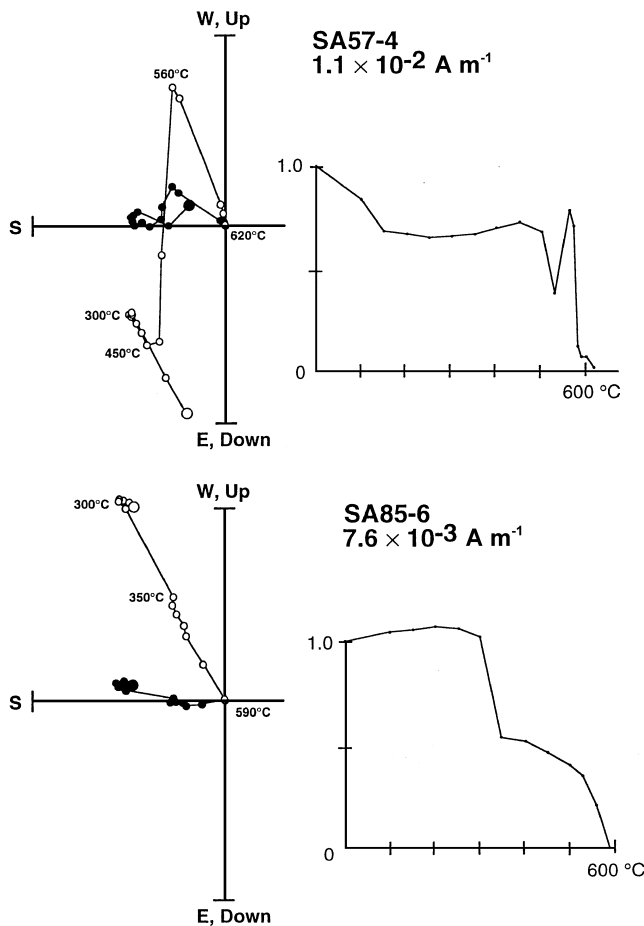


Figure 3. Orthogonal projections and thermal demagnetization curves of anomalous thermal demagnetization behaviour for specimens in the sites of SA57 and SA85. Four-component magnetization is observed in specimens of SA57. An abrupt decrease of remanent intensity appears between 300 and 350 °C in specimens of SA85. This is indicative of the presence of pyrrhotite or maghemite.

in the Kema area instead shows clockwise deflection in declination ($D = 192.2^\circ$, $I = -56.9^\circ$) (Otofujii *et al.* 2002). These facts and non-negative results of the bedding-tilt test suggest that no sites showing a southeasterly direction with reversed polarity are excluded on the basis of overprinted magnetization.

A mean direction for the whole Sikhote Alin at the reference point (44°N , 135°E) is calculated (Table 1); a palaeomagnetic pole is calculated from a mean palaeomagnetic direction of each sampling site, then the palaeomagnetic direction at the reference point within Sikhote Alin (44°N , 135°E) is inversely calculated from the pole, and the mean direction is obtained. Two data sets are used for the calculation: whole data from 39 sites and the selected 25 data from four areas (Kema river, Terney, Plastun and Moryak-Rybolov) where each data set passes the positive bedding-tilt test or reveals an increase in precision of the parameter after tilt correction.

The tilt-corrected mean direction from the selected 25 sites reveals counterclockwise deflection from the north: $D = 331.1^\circ$, $I = 53.5^\circ$ ($\alpha_{95} = 8.5^\circ$, $k = 12.7$) ($N = 25$). The precision parameter k increases from 7.9 to 12.7. However, the increase is critically insufficient to yield the positive fold test of McElhinny (1964) even at the 95 per cent level ($12.7/7.9 = 1.61 < F_{48,48} = 1.62$). We have also applied the bedding-tilt test of McFadden (1990) to the mean palaeomagnetic directions. The calculated value for ξ_1 is 12.9

in the *in situ* coordinates and ξ_1 is 3.47 after tilt correction, while the critical value at the 95 per cent confidence level is $\xi_c = 5.82$. This bedding-tilt test demonstrates that the hypothesis that these magnetizations were acquired *in situ* can be rejected at the 95 per cent confidence level. Alternatively, a tilt-corrected mean direction from all 39 sites also reveals a counterclockwise deflection from the north: $D = 335.6^\circ$, $I = 54.4^\circ$ ($\alpha_{95} = 8.5^\circ$, $k = 8.3$) ($N = 39$). The bedding-tilt test of McFadden (1990) shows positive at the 99 per cent confidence level; the calculated value for ξ_1 is 20.3 in the *in situ* coordinates and ξ_1 is 5.22 after tilt correction, while the critical value at the 99 per cent confidence level is $\xi_c = 10.3$. It is thus apparent that the Late Cretaceous Kisin Group of Sikhote Alin acquired its magnetization during some period prior to the tilting. Because the two mean directions are not indistinguishable and the sampling localities of the whole data set cover a wider region than that of the selected data set, the mean direction of 39 sites provides a first-order approximation for the characteristic palaeomagnetic direction for Sikhote Alin.

We also applied the reversal test of McFadden & McElhinny (1990) to the whole 39 data sets. γ_c is 16.3° from data sets of normal and reversed directions, so that these data sets are classified as a class 'C' reversal test. The difference between normal and reversed mean directions is 159.1° . Although these data sets do not pass the reversal test according to the criterion of McFadden & McElhinny (1990), it should be noted that this result is only just less than the critical angle of 160° . This result is probably caused by the easterly directions from the Kuznetsovo area, since data sets excluding these data pass the reversal test. The presence of two polarities of probable primary origin implies that the Kisin Group records the geomagnetic field over a fairly long period.

Taking into account the results of the reliability from the tests described above, we consider that the mean direction computed at the whole data set is the characteristic palaeomagnetic direction of the Late Cretaceous Kisin Group in Sikhote Alin. A mean palaeomagnetic pole for Sikhote Alin is computed from 39 site poles calculated from site mean palaeomagnetic directions and is located at 71.5°N , 38.9°E ($A_{95} = 9.9^\circ$).

4 ANISOTROPY OF MAGNETIC SUSCEPTIBILITY

Anisotropy of magnetic susceptibility measurements were performed on specimens using a Kappabridge KLY-3 apparatus. Although the anisotropy of magnetic susceptibility (AMS) ($K_{\text{max}}/K_{\text{min}} - 1$) reveals a wide range between 2 and 26 per cent, oblate susceptibility ellipsoids dominate most specimens. The principal directions (maximum, intermediate and minimum axes; K_{max} , K_{int} and K_{min} , respectively) are calculated for each specimen.

Fig. 5 shows the principal directions in a stratigraphic coordinate system and lineation/foliation diagrams for samples of the Kema river and Moryak-Rybolov areas. The AMS of the Kema river area is less than 3 per cent, whereas that for Moryak-Rybolov sites reaches up to 26 per cent. Magnitude of anisotropy is generally related to intensity of magnetic susceptibility; the mean magnetic susceptibilities of the Kema river sites and Moryak-Rybolov sites are 1.4×10^{-4} and 7.7×10^{-3} SI units, respectively. The magnetic fabrics of both areas are characterized by an oblate susceptibility ellipsoid. The minimum axes of the majority of specimens are nearly parallel to the vertical axis in stratigraphic coordinates, indicating that the depositional origin of the welded tuffs is preserved. There are no apparent correlations between directions of remanent magnetization and the maximum axes of susceptibility in each area. Since

Kisin Group

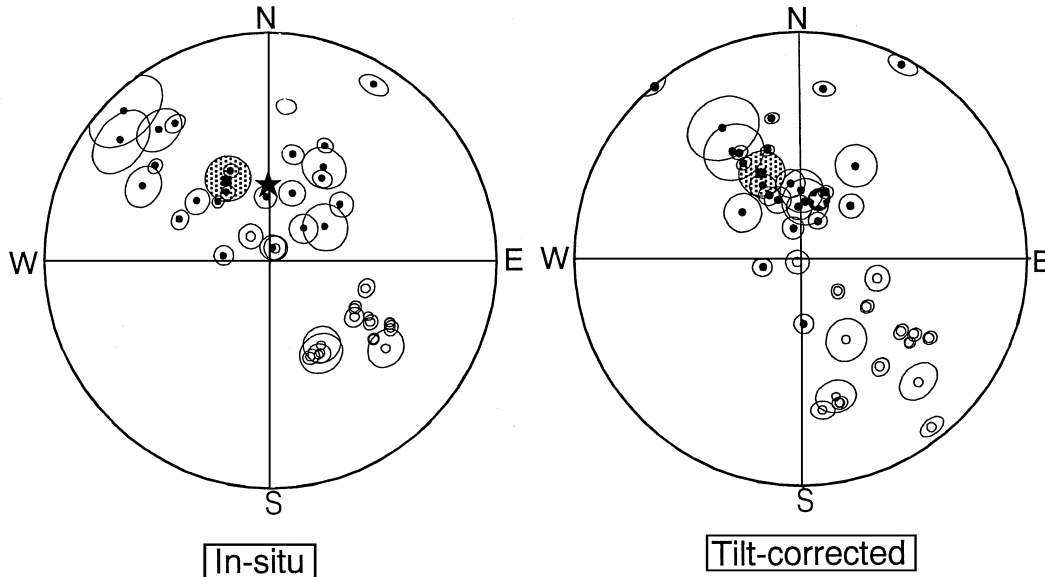


Figure 4. Equal-area projections of the site mean directions with their 95 per cent circles of confidence for the Kisin Group. Site mean directions of 39 sites are shown before and after tilt correction. A square with a shaded 95 per cent circle of confidence indicates the overall mean direction. The Fisherian precision parameter, k , and the radius of the 95 per cent cone of confidence, α_{95} , change from ($k = 7.6$, $\alpha_{95} = 8.9^\circ$) to ($k = 8.3$, $\alpha_{95} = 8.5^\circ$) after tilt adjustment. A star in *in situ* coordinates indicates the direction of geocentric axial dipole field. Star in tilt-corrected coordinate indicates the expected 70 Ma direction ($D = 16.8^\circ$, $I = 67.1^\circ$) computed from the coeval reference pole (77.2°N , 192.4°E) (Besse & Courtillot 1991). Solid symbols for the lower hemisphere, open symbols for the upper hemisphere.

inclinations of palaeomagnetic directions for the Moryak-Rybolov area are steeper than those of the Kema river area, strong AMS does not give rise to inclination shallowing. These results indicate that directions of remanent magnetization are not controlled by the alignment of anisotropic minerals in the studied welded tuffs.

5 DISCUSSION

5.1 Counterclockwise rotation of Sikhote Alin

The most significant result in this study is the counterclockwise deflection of the palaeomagnetic direction of the Kisin Group, which characterizes all areas except Kuznetsovo. The declination of the mean palaeomagnetic direction ($D = 335.6^\circ$) is rotated by 41.4° from that of the palaeomagnetic direction ($D = 16.8^\circ$, $I = 67.1^\circ$) expected from the 70 Ma Eurasian reference pole (77.2°N , 192.4°E , $A_{95} = 4.1^\circ$) (Besse & Courtillot 1991) (Fig. 4). This is also discernible from the distribution of poles calculated from the Kisin Group and the reference apparent polar wander path (APWP) of Eurasia (Besse & Courtillot 1991; Van der Voo 1993) (Fig. 6). Because palaeomagnetic directions from the Kisin Group reveal both normal and reversed polarities, this difference in declination cannot be caused by transient geomagnetic behaviours but is attributed to a tectonic rotation of the Sikhote Alin mountain range. The uncertainty in this rotation is evaluated as 16.0° , according to the formulae of Magill *et al.* (1981). We therefore propose that Sikhote Alin was subjected to a counterclockwise rotation of the order of $41^\circ \pm 16^\circ$ with respect to the remaining part of the Eurasian continent after the Late Cretaceous. Counterclockwise rotation is observed over an area extending, at least, from 43.4°N to 46.4°N latitude (Fig. 1) in the Sikhote Alin mountain range.

Fig. 6 shows the palaeomagnetic poles from the Sijanov Group and the Bogopol Group (Otofujii *et al.* 1995) and the great circle

running through the reference point of Sikhote Alin (44°N , 135°E) and the 50 Ma Eurasian reference pole. We note a decrease in the amount of rotation with respect to Eurasia from the Kisin, through the Sijanov and to the Bogopol poles, although the Sijanov pole has a large A_{95} . No significant clockwise rotation ($8.5^\circ \pm 17.0^\circ$) is detected in the youngest Bogopol Group (Otofujii *et al.* 1995; Besse & Courtillot 1991). This statistically insignificant rotation indicates that counterclockwise rotation of the area, which is supported by Kisin and Sijanov poles, had ended by 53–50 Ma.

Rotation models of blocks at continental margins fall broadly into two categories (e.g. Randall 1998); comprising small-scale *in situ* rotation and large-scale rigid rotation. Uno *et al.* (1999) attribute the counterclockwise rotation of the study areas in Sikhote Alin to the former category. Sinistral strike-slip movement on the Central Sikhote Alin Fault is considered to be responsible for the *in situ* rotation of blocks comprising Sikhote Alin. Displacements of 60–250 km (Natal'in *et al.* 1986; Natal'in 1993) are considered to be large enough to cause rotation for blocks bounded by secondary small faults.

However, an alternative explanation in terms of a large-scale rigid rotation may be required, because a counterclockwise rotation of $36^\circ \pm 17^\circ$ with respect to the Eurasian continent is observed in the Chinese territory from Qitaihe in Heilongjiang province (45.8°N , 131.0°E) (Uchimura *et al.* 1996) where Late Jurassic to Early Cretaceous sandstones and welded tuffs show a westerly palaeomagnetic direction ($D = 338.8^\circ$, $I = 65.6^\circ$, $\alpha_{95} = 6.2^\circ$) (Fig. 7). The geographical extent of the area affected by counterclockwise rotation suggests that it applies to the whole eastern part of the Mongolia Block.

The block rotation of Sikhote Alin could be related to the development of extensional basins in the interior of the Asian continent (Fig. 1). The Middle Amur basin, located along the lower stream of the present Amur river, extends SW–NE and is 400 km long and 200 km

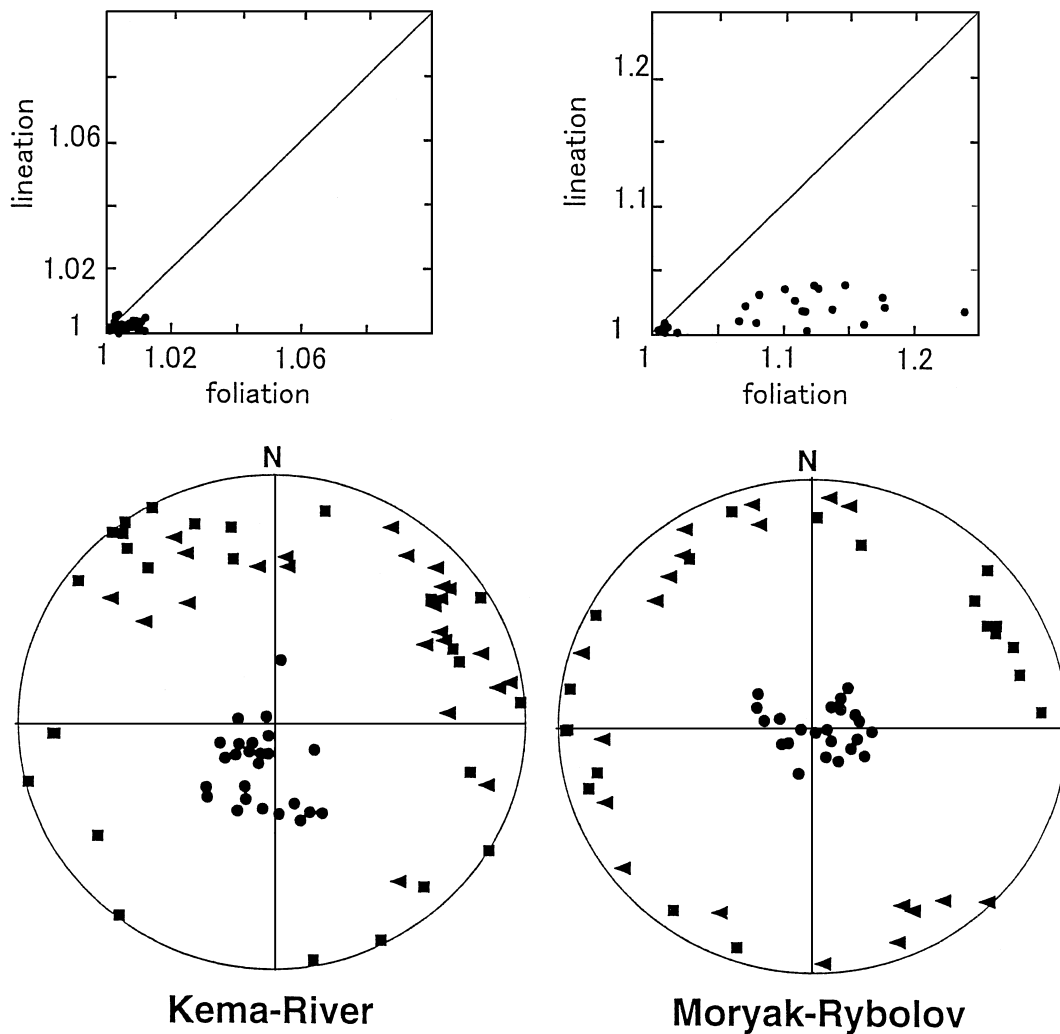


Figure 5. Magnetic lineation/foiliation diagrams and the principal directions of susceptibility of the Kema river and Moryak-Rybolov areas for the Kisin Group. Magnetic lineation and foliation are defined as K_{\max}/K_{int} and K_{int}/K_{\min} , respectively. The principal directions are projected on to the lower hemisphere in a stratigraphic coordinate system (equal-area projection). Squares are K_{\max} (maximum susceptibility direction); triangles are K_{int} (intermediate susceptibility directions); circles are K_{\min} (minimum susceptibility directions).

wide. The commencement of continental sedimentation is estimated to be Santonian to Campanian in age (Kirillova 1995). This basin extends southward and forms the Sanjiang Cenozoic faulted graben belts in which faulting and block-faulting were extensive during Cretaceous times (Bureau of Geology and Mineral Resources of Heilongjiang Province 1993). The Hulin area on the northern coast of Xanka lake was also the site of active block-faulting during the Late Cretaceous, and converted to a faulted graben belt in Cenozoic times. This basin extends into the Razdolnian rifts.

Large Cretaceous basins are distributed into the interior further west from the Middle Amur–Sanjian–Razdolnian basins. Lacustrine-alluvial sedimentation commenced at approximately 90 Ma in the Amur-Zeya Basin and to the south, the wide Songliao basin extends SW–NE (Fig. 1). The development of these basins occurred in Late Early Cretaceous to Late Cretaceous times and large subsidence followed faulting (Yang *et al.* 1986). The tectonic activity represented by these rifts and faulted belts is interpreted to be a consequence of the counterclockwise rotation of both the Sikhote Alin Block and Qitaihe area of Heilongjiang province.

5.2 Differential rotation between the eastern part of the Mongolia Block and the eastern part of the NCB

While counterclockwise rotation occurred in the eastern part of the Mongolia Block, the eastern part of the NCB including the Korean peninsula was subjected to clockwise rotation during the Cretaceous (Ma *et al.* 1993; Uchimura *et al.* 1996) (Fig. 7). Palaeomagnetic investigations in the Korean Peninsula suggest that clockwise rotation of 11° – 36° occurred later than the Aptian (Upper Lower Cretaceous) (Zhao *et al.* 1999; Uno 2000). A comparable clockwise rotation is also reported in the Benxi area (41.3°N , 123.8°E) (Uchimura *et al.* 1996). Indeed, Uchimura *et al.* (1996) suggest a post-Cretaceous clockwise rotation of $17.9^{\circ} \pm 9.8^{\circ}$ of the Liaoning Province (east of the Tan-Lu fault TLF) with respect to the united NCB–SCB west of the TLF.

These palaeomagnetic results show that the eastern margin of the Mongolia Block and the NCB experienced differential rotations after the Mesozoic with the eastern part of the Mongolia Block rotating counterclockwise and the eastern part of the NCB rotating

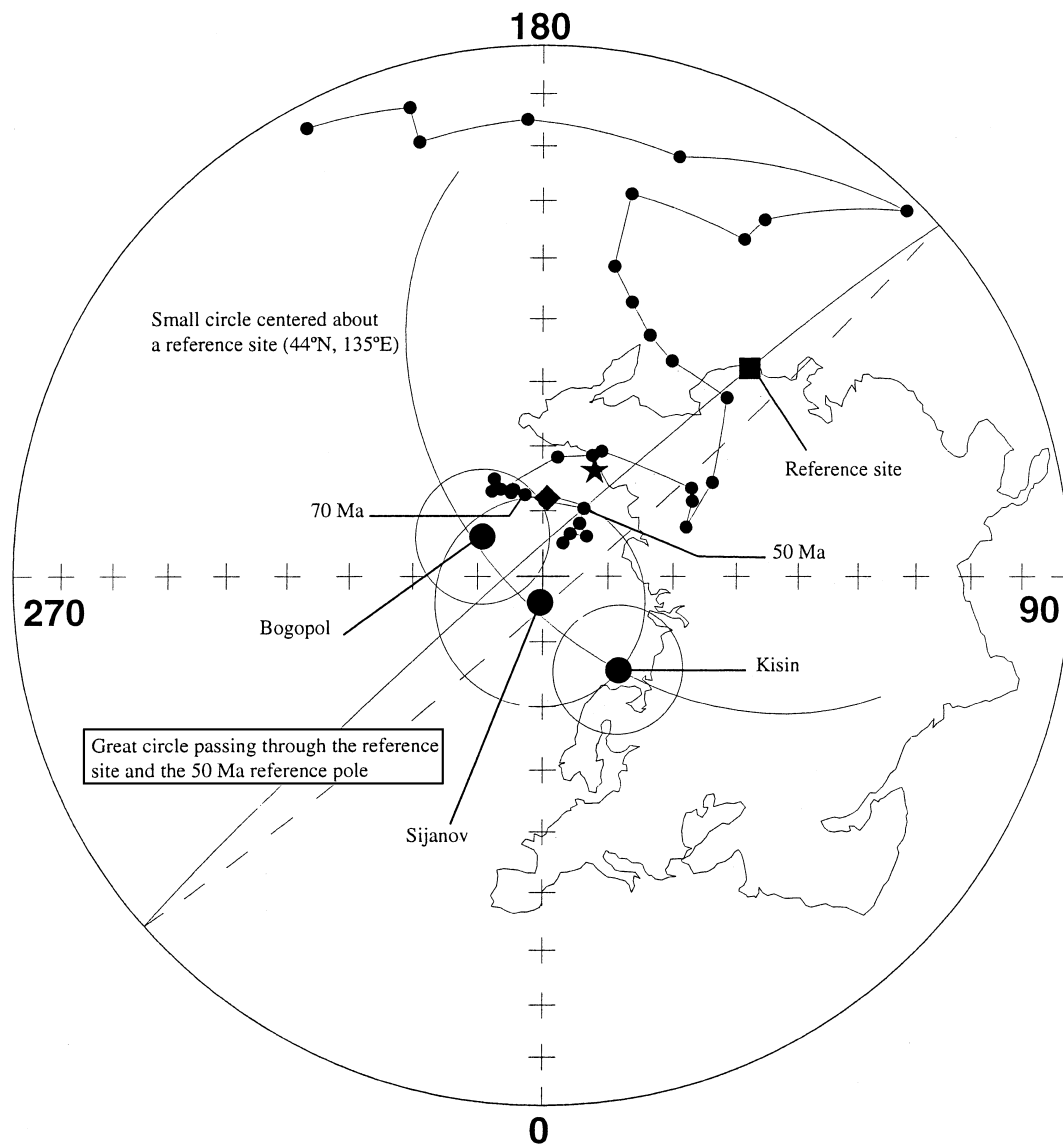


Figure 6. Palaeomagnetic poles (with associated circles of 95 per cent of confidence) of the Kisin Group compared with the reference apparent polar wander (Besse & Courtillot 1991). The Sijanov and Bogopol poles obtained from Sikhote Alin (Otofuji *et al.* 1995) are also drawn. Eurasian poles (with associated circles of 95 per cent of confidence) for the Late Cretaceous (star) and the Palaeogene (diamond) are after Van der Voo (1993). A small circle centred on the reference site (44°N , 135°E) of Sikhote Alin is projected through the Kisin pole. The great circle runs through the reference site and the 50 Ma reference pole (polar stereographic projection).

clockwise. This differential rotational is analogous to the Miocene rifting of the Japanese islands associated with the opening of the Japan Sea. Indeed, a counterclockwise rotation occurred in NE Japan, whereas a clockwise rotation took place in SW Japan (Otofuji *et al.* 1985). Differential rotation of two blocks extending north–south has therefore occurred at least twice along the eastern margin of the Asian continent since the Late Mesozoic.

We suggest that a net horizontal force toward the ocean side is responsible for the displacement and the block rotation at the eastern margin of the Asian continent. The oceanward net force would have concentrated on the area between the southern part of the eastern margin of the Mongolia block and the northern part of the eastern margin of the NCB and brought about differential rotation between these two blocks (Fig. 7c). As the eastern part of the Asian continent was formed by the collision of Siberia and the Mongolia–NCB blocks between the Late Carboniferous and Middle Jurassic

(Zonenshain *et al.* 1990), and by the collision of the NCB and Yangtze block between the Permian and Early Cretaceous (Yokoyama *et al.* 2001), generation of the oceanward net force is possibly correlated with the collision history of these blocks.

We emphasize the importance of mantle flow below the eastern Asian continental margin to explain intermittent generation of a net horizontal force toward the ocean side, although extension along the eastern margin of Eurasia has been variously ascribed to hot cells (Miyashiro 1986), plumes (Nakamura *et al.* 1989) and variation of Pacific–Eurasia convergence rate (Northrup *et al.* 1995). Numerical experiments suggest that small subcontinental upwellings intermittently occur next to the continental margin after the growth of a mega-continent by a collision of two continents (Lowman & Jarvis 1996). 2-D mantle convection flow (Gurnis 1988; Lowman & Jarvis 1996; Honda *et al.* 2000) is a possible source for the intermittent tectonics, which has occurred at the Asian continental margin

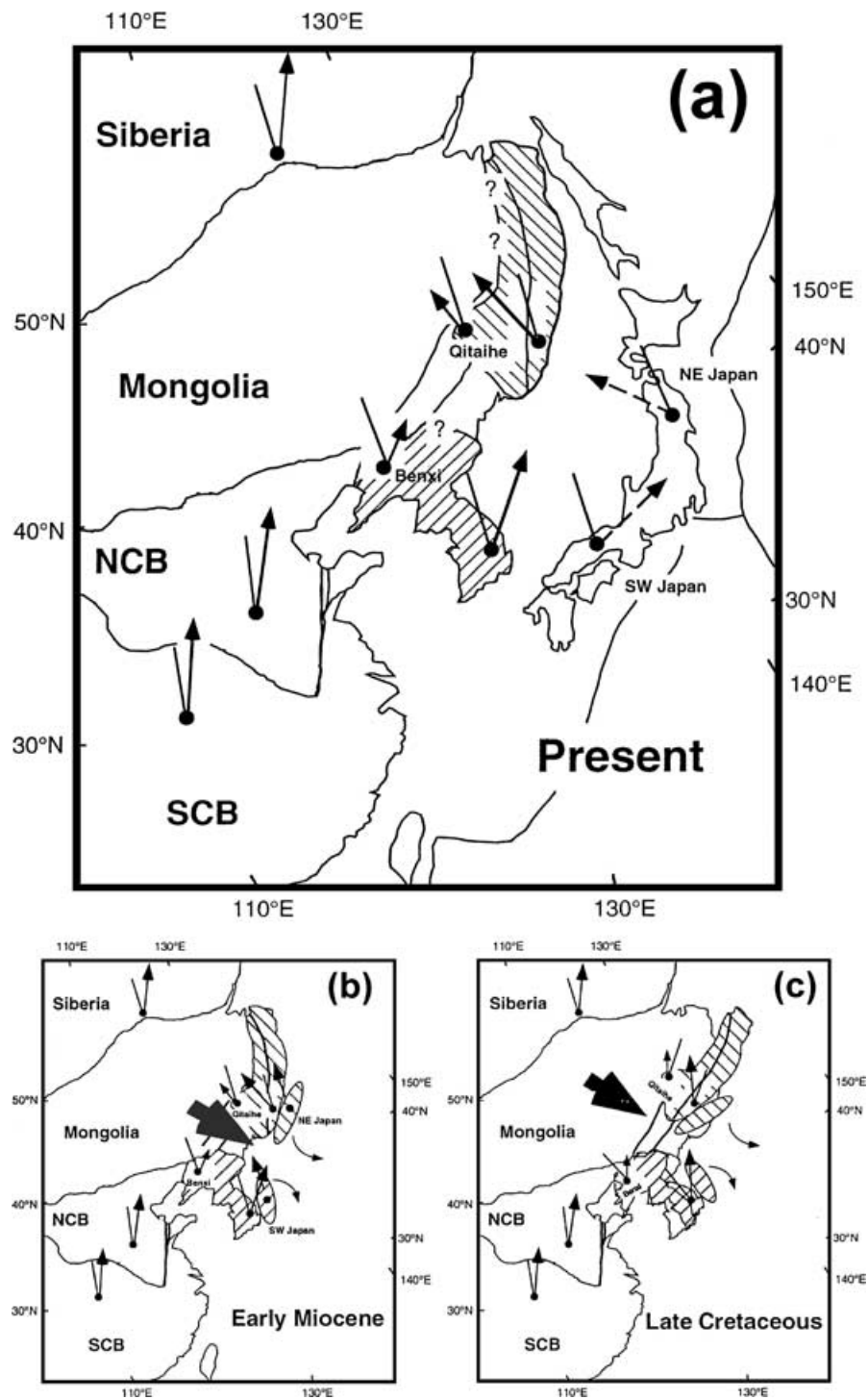


Figure 7. Cretaceous palaeomagnetic directions and tectonic model in the eastern margin of Asia. (a; present) The Late Cretaceous palaeomagnetic direction of Sikhote Alin is the mean direction of the Kisin Group. Early Cretaceous directions in the Korean Peninsula are after Zhao *et al.* (1999). Cretaceous palaeomagnetic directions of Benxi and Qitaihe are after Uchimura *et al.* (1996). Cretaceous palaeomagnetic directions are calculated for Siberia (120°E, 58°N) from the 70 Ma pole of Besse & Courtillot (1991), for the NCB (115°E, 35°N) from the Cretaceous pole of Gilder & Courtillot (1997) and for the SCB (10°E, 30°N) from the Late Cretaceous pole of Zhao *et al.* (1996). Palaeomagnetic directions of the Japanese islands are Early Miocene (Otofuji *et al.* 1985). Counterclockwise rotation recorded in Sikhote Alin extends to the interior of the Mongolia block, and clockwise rotation area extends from the Korean Peninsula to its root in the NCB. (b; Early Miocene) The Japanese islands are reconstructed to a position prior to opening of the Japan Sea. The oceanward net force (arrow) caused Northeast Japan to rotate counterclockwise and Southwest Japan to rotate clockwise associated with the opening of the Japan Sea at approximately 15 Ma. (c; Late Cretaceous) Sikhote Alin and Korean peninsula are reconstructed by clockwise rotation through 41° and counterclockwise rotation through 22°, respectively, to bring Cretaceous palaeomagnetic directions into parallelism with the interior of the Asian continent. A net horizontal force towards the ocean side (arrow) acted on the lithosphere of the eastern margin of the Asian continent in the Late Cretaceous to Palaeocene. The eastern marginal parts of the Mongolia Block and NCB experienced differential rotation; the eastern part of the Mongolia Block rotated counterclockwise and the eastern part of the NCB clockwise in the Late Cretaceous.

after complete suturing of the Siberia–Mongolia–NCB–SCB blocks. Upwelling of deep-seated mantle material is discovered in Sikhote Alin and Japanese islands during the rifting of the Japanese islands (Nohda *et al.* 1988; Okamura *et al.* 1998), and in northeast China (Hannuoba, Kundian) during the Cenozoic volcanic activity (Song *et al.* 1990; Tatsumoto *et al.* 1992).

A northward push from the southern part of Asia is an alternative possibility for Late Cretaceous differential rotation at the eastern Asian margin, because the Lhasa block and the Indian continent successively collided with the southern margin of Asia in Mesozoic and Cenozoic times. The extrusion model using a thin-shell numerical model (Kong *et al.* 1997) cannot explain the counterclockwise rotation of the eastern part of the Mongolia Block.

5.3 Shallow magnetizations of Late Cretaceous and Palaeocene age in Sikhote Alin

The second significant feature of the magnetization in Sikhote Alin is the shallow inclination. In Fig. 6, palaeomagnetic poles from Sikhote Alin are compared with the reference apparent polar wander path of Eurasia (Besse & Courtillot 1991). We plot the small circle centred about the reference site (44°N, 135°E) containing the pole of the Kisin Group to show that palaeomagnetic poles from Sikhote Alin are far-sided with respect to the reference APWP. The far-sided position is also observed with respect to the European Cretaceous and Palaeogene poles that plot at 72°N, 154°E and 78°N, 177°E (Van der Voo 1993). Observed inclination values at the reference site of Sikhote Alin are shallower than those expected from the 70 or 50 Ma reference poles by $12.7^\circ \pm 9.2^\circ$ for the Kisin Group, $11.5^\circ \pm 12.0^\circ$ for the Sijanov Group and $13.5^\circ \pm 9.2^\circ$ for the Bogopol Group, respectively.

Anomalously low inclinations have been reported from Tertiary rocks of the Asian continent (Chauvin *et al.* 1996; Cogné *et al.* 1999), since Westphal *et al.* (1986) noticed the low palaeolatitude in the Tethyan mobile belt at Eocene and Oligocene times. Our study indicates that shallow inclination in the eastern part of the Asian continent appears at Late Cretaceous and Tertiary times. According to a compilation of palaeomagnetic data from Russia (Khramov *et al.* 1990), Upper Cretaceous rocks preserve low inclinations in the Transbaikal, Great Hingan Mountains and Sakhalin in the Mongolia Block.

The low inclination in the eastern part of the Asian continent has been attributed to either the nature of the geomagnetic field or to large-scale tectonic motions. The former possibility is accommodated by a northward offset of the axial dipole (Wilson 1971). A stationary non-dipole component beneath the Mongolia Block could also be responsible for the Cretaceous palaeomagnetic directions in the Mongolia Block and Palaeogene palaeomagnetic directions from central and eastern Asia (Chauvin *et al.* 1996). The Mongolian anomaly remains stationary in central Asia at the present time (Yukutake & Tachinaka 1968).

Arguments in favour of northward movement of eastern Asia are based largely on Cretaceous to Palaeogene palaeomagnetic data from Korea and Japan (Lee *et al.* 1987; Otofujii 1996). This northward movement would have ceased by 10 Ma because of good agreement of pole positions from eastern Asia and Eurasia (Besse & Courtillot 1991; Otofujii *et al.* 1991; Enkin *et al.* 1992; Otofujii 1996). A non-rigid behaviour of the Eurasian continent was proposed as a tentative solution (Cogné *et al.* 1999) to reconcile low inclinations in Palaeogene rocks distributed through central Asia. However, the SCB seems to have been united with Eurasia by the Late Creta-

ceous because Late Cretaceous palaeomagnetic poles from the SCB (Enkin *et al.* 1992; Zhao *et al.* 1996; Gilder & Courtillot 1997) are compatible with the 70 Ma pole from Eurasia (Besse & Courtillot 1991). The better observation led Halim (1998) and Cogné *et al.* (1999) to question the validity of including Siberia in the APWP of Besse & Courtillot (1991) prior to the Tertiary. However, since the Mongolia Block appeared to have been welded to the NCB–SCB blocks by the Early Cretaceous (Gilder *et al.* 1999), models involving independent northward movement of the Mongolia Block are difficult to support. The hypothesis of large-scale northward movement of the Mongolia–NCB–SCB blocks has still to be tested by reliable Cretaceous palaeomagnetic data from eastern Asia, including the Siberia Block.

6 CONCLUSION

The study of the Late Cretaceous Kisin Group from Sikhote Alin provides 39 reliable palaeomagnetic directions from eight areas ranging from 46.7°N, 138.1°E to 43.4°N, 134.9°E. The tilt-corrected mean direction of the data set of whole 39 sites is $D = 335.6^\circ$, $I = 54.4^\circ$ ($\alpha_{95} = 8.5^\circ$). This direction is not indistinguishable from the mean direction ($D = 331.1^\circ$, $I = 53.5^\circ$, $\alpha_{95} = 8.5^\circ$) based on the selected 25 sites from four areas (Kema river, Terney, Plastun and Moryak-Rybolov) with more reliable data sets. We conclude that the mean direction of 39 sites is the characteristic palaeomagnetic direction for Sikhote Alin, because the sampling localities of 39 sites cover a wider region than that of the selected 25 sites. Palaeomagnetic declination indicates that the Sikhote Alin Block rotated counterclockwise through $41^\circ \pm 16^\circ$ with respect to the Eurasian continent between Late Cretaceous times and 53–50 Ma. Taken together with the clockwise rotation of the eastern part of the NCB, differential rotational motions are observed in the eastern margin of the Asian continent during the Late Cretaceous. This could have been a consequence of a net horizontal force towards the east acting on the lithosphere at the eastern margin of the Asian continent or episodic collisional history of blocks to the south. We suggest that intermittently occurring upwellings of the mantle and associated horizontal flows at the base of the continental plate were responsible.

ACKNOWLEDGMENTS

The efficient field logistics were set up by the Pacific Oceanological Institute (POI). We are grateful to B. Stolov, V. M. Nikiforov, L. Kulchitskaja, Y. Pochkay, E. P. Radchenko and M. V. Radchenko for help on sampling in the field. Zhenyu Yang reviewed an early version of the manuscript. We also thank B. Harbert, P. Roperch, J.-C. Thomas, M. Bazhenov, R., Russo, J. Piper, P.L. McFadden and an anonymous reviewer for the critical reviews that helped us to improve the manuscript. This work was supported in part by the Hyogo Science and Technology Association, and Grant-in-aid (nos 08041110, 09041109, 11691129, 14403010) from the Japanese Ministry of Education, Science and Culture.

REFERENCES

- Besse, J. & Courtillot, V., 1991. Revised and synthetic apparent polar wander paths of the African, Eurasian, North American and Indian Plates, and true polar wander since 200 Ma, *J. geophys. Res.*, **96**, 4029–4050.
- Bretstein, Y.S., 1988. Magnetic properties of Late Cretaceous–Cenozoic volcanic rocks of the Soviet Far East South, *J. Phys. Earth*, **36**, S39–S64.

- Bureau of Geology and Mineral Resources of Heilongjiang Province, 1993. *Regional geology of Heilongjiang Province, Geological memoirs, Series 1*, p. 734, Geol. Publishing House, Beijing.
- Chauvin, A., Perroud, H. & Bazhenov, M.L., 1996. Anomalous low palaeomagnetic inclinations from Oligocene-Lower Miocene red beds of the south-west Tien Shan, Central Asia, *Geophys. J. Int.*, **126**, 303–313.
- Cogné, J.P., Halim, N., Chen, Y. & Courtillot, V., 1999. Resolving the problem of shallow magnetizations of Tertiary age in Asia: insights from paleomagnetic data from the Qiangtang, Kunlun, and Qaidam blocks (Tibet, China), and a new hypothesis, *J. geophys. Res.*, **104**, 17 715–17 734.
- Enkin, R.J., Yang, Z.Y., Chen, Y. & Courtillot, V., 1992. Paleomagnetic constraints on the geodynamic history of the major blocks of China from the Permian to the Present, *J. geophys. Res.*, **97**, 13 953–13 989.
- Faure, M., Natal'in, B.A., Monié, P., Vrublevsky, A.A., Borukaiev, Ch. & Prikhodko, V., 1995. Tectonic evolution of the Anuy metamorphic rocks (Sikhote Alin, Russia) and their place in the Mesozoic geodynamic framework of East Asia, *Tectonophysics*, **241**, 279–301.
- Gilder, S. & Courtillot, V., 1997. Timing of the North–South China collision from new middle to late Mesozoic paleomagnetic data from the North China Block, *J. geophys. Res.*, **102**, 17 713–17 727.
- Gilder, S. *et al.*, 1999. Tectonic evolution of the Tancheng-Lujiang (Tan-Lu) fault via Middle Triassic to Early Cenozoic paleomagnetic data, *J. geophys. Res.*, **104**, 15 365–15 390.
- Golozubov, V.V. & Khanchuk, A.I., 1996. Taukha and zhuravlevka terranes of the south Sikhote Alin—fragments of the early cretaceous margin of Asia, *Geol. Pac. Ocean*, **12**, 203–220.
- Gurnis, M., 1988. Large-scale mantle convection and the aggregation and dispersal of supercontinents, *Nature*, **332**, 695–699.
- Halim, N., 1998. Contribution du Paléomagnétisme à la compréhension de la tectonique post-collision entre inde et Sibérie, *Doctor's thesis*, l'Institut de Physique du Globe de Paris.
- Honda, S., Yoshida, M., Ootorii, S. & Iwase, Y., 2000. The timescale of plume generation caused by continental aggregation, *Earth planet. Sci. Lett.*, **176**, 31–43.
- IAGA Division V, Working Group 8, 1995. International geomagnetic reference field, 1995 revision, *J. Geomag. Geoelectr.*, **47**, 1257–1261.
- Khranov, A.N., Petrova, G.N. & Pechersky, D.M., 1990. Paleomagnetism of the Soviet Union, in *Paleoreconstruction of the Continents*, Geodyn. Ser., Vol. 2, pp. 177–194, eds McElhinny, M.W. & Valencio, D.A., AGU, Washington, DC.
- Kirillova, G.L., 1995. Late Mesozoic environmental history of south-eastern Russia, in *Environmental and Tectonic History of East and South Asia*, 15th Int. Symp. Proc. of Kyungpook National University, pp. 93–107.
- Kirschvink, J.L., 1980. The least-squares line and plane and the analysis of palaeomagnetic data, *Geophys. J. R. astr. Soc.*, **62**, 699–718.
- Kong, X., Yin, A. & Harrison, T.M., 1997. Evaluating the role of preexisting weaknesses and topographic distributions in the Indo-Asia collision by use of a thin-shell numerical model, *Geology*, **25**, 527–530.
- Krassilov, V.A., 1990. *Continental Cretaceous of the USSR*, p. 224, USSR Academy of Science, Far East Branch, Vladivostok.
- Lee, G., Besse, J., Courtillot, V. & Montigny, R., 1987. Eastern Asia in the Cretaceous: new paleomagnetic data from South Korea and a new look at Chinese and Japanese data, *J. geophys. Res.*, **92**, 3580–3596.
- Lowman, J.P. & Jarvis, G.T., 1996. Continental collisions in wide aspect ratio and high Rayleigh number two-dimensional mantle convection models, *J. geophys. Res.*, **101**, 25 485–25 497.
- Ma, X.H., Yang, Z.Y. & Xing, L.S., 1993. The Lower Cretaceous reference pole for North China, and its tectonic implications, *Geophys. J. Int.*, **115**, 323–331.
- Magill, J., Cox, A. & Duncan, R., 1981. Tillamook volcanic series: further evidence for tectonic rotation of the Oregon Coast Range, *J. geophys. Res.*, **86**, 2953–2970.
- Matsuda, T., Sakiyama, T., Enami, R., Otofujii, Y., Sakhno, V.G., Matunin, A.P., Kulnich, R.G. & Zimin, P.S., 1998. Fission-track ages and magnetic susceptibility of Cretaceous to Paleogene volcanic rocks in southeastern Sikhote Alin, Far East Russia, *Res. Geol.*, **48**, 285–290.
- Matyunin, A.P., 1988. Magmatism evolution of Kavalеровskaya ore-magmatic system, in *Magmatism of Ore Areas and Knots (Pri-morye)*, pp. 83–88, USSR Academy of Sciences, Far-Eastern Branch, Vladivostok.
- McElhinny, M.W., 1964. Statistical significance of the fold test in palaeomagnetism, *Geophys. J. R. astr. Soc.*, **8**, 338–340.
- McFadden, P.L., 1990. A new fold test for palaeomagnetic studies, *Geophys. J. Int.*, **103**, 163–169.
- McFadden, P.L. & McElhinny, M.W., 1990. Classification of the reversal test in palaeomagnetism, *Geophys. J. Int.*, **103**, 725–729.
- Miki, M., 1995. Two phase opening model for the Okinawa Trough inferred from paleomagnetic study of the Ryukyu arc, *J. geophys. Res.*, **100**, 8169–8184.
- Miyashiro, A., 1986. Hot regions and the origin of marginal basins in the western Pacific, *Tectonophysics*, **122**, 195–216.
- Nakamura, E., Campbell, I.H., McCulloch, M.T. & Sun, S.S., 1989. Chemical geodynamics in a back-arc region around the Sea of Japan: Implications for the genesis of alkaline basalts in Japan, Korea and China, *J. geophys. Res.*, **94**, 4634–4654.
- Natal'in, B., 1993. History and modes of Mesozoic accretion in Southeastern Russia, *Island Arc*, **2**, 15–34.
- Natal'in, B.A., Parfenov, L.M., Vrublevsky, A.A., Karaskov, L.P. & Yushmanov, V.V., 1986. Main fault systems of the Soviet Far East, *Phil. Trans. R. Soc. Lond.*, A., **317**, 267–275.
- Nohda, S., Tatsumi, Y., Otofujii, Y., Matsuda, T. & Ishizaka, K., 1988. Asthenospheric injection and back-arc opening: isotopic evidence from northeast Japan, *Chem. Geol.*, **68**, 317–327.
- Northrup, C.J., Royden, L.H. & Burchfiel, B.C., 1995. Motion of the Pacific plate relative to Eurasia and its potential relation to Cenozoic extension along the eastern margin of Eurasia, *Geology*, **23**, 719–722.
- Okamura, S., Arculus, R.J., Martynov, Y.A., Kagami, H., Yoshida, T. & Kawano, Y., 1998. Multiple magma sources involved in marginal-sea formation: Pb, Sr. and Nd isotopic evidence from the Japan Sea region, *Geology*, **26**, 619–622.
- Otofujii, Y., 1996. Large tectonic movement of the Japan Arc in Late Cenozoic times inferred from paleomagnetism: review and synthesis, *Island Arc*, **5**, 229–249.
- Otofujii, Y., Itaya, T. & Matsuda, T., 1991. Rapid rotation of southwest Japan—palaeomagnetism and k-Ar ages of Miocene volcanic rocks of southwest Japan, *Geophys. J. Int.*, **105**, 397–405.
- Otofujii, Y., Matsuda, T. & Nohda, S., 1985. Opening mode of the Japan Sea inferred from the palaeomagnetism of the Japan Arc, *Nature*, **317**, 603–604.
- Otofujii, Y. *et al.*, 1995. Late Cretaceous to early Paleogene paleomagnetic results from Sikhote Alin, Far Eastern Russia: implications for deformation of East Asia, *Earth planet. Sci. Lett.*, **130**, 95–108.
- Otofujii, Y. *et al.*, 2002. Internal deformation of Sikhote Alin volcanic belt, far eastern Russia: Paleocene paleomagnetic results, *Tectonophysics*, **350**, 181–192.
- Pullaiah, G., Irving, E., Buchan, K.L. & Dunlop, D.J., 1975. Magnetization changes caused by burial and uplift, *Earth planet. Sci. Lett.*, **28**, 133–143.
- Randall, D.E., 1998. A new Jurassic–Recent apparent polar wander path for South America and a review of central Andean tectonic models, *Tectonophysics*, **299**, 49–74.
- Sakhno, V.G., Matyunin, A.P., Martynov, Yu. A., Popov, V.K. & Polin, V.F., 1991. East-Sikhote-Alinsky volcanic belts, in *Magmatism of Asian Eastern Margin*, pp. 99–110, eds Sheglov, A.D. & Zimin, S.S., Nauka, Moscow.
- Song, Y., Frey, F.A. & Zhai, X., 1990. Isotopic characteristics of Hannuoba basalts, eastern China: implications for their petrogenesis and the composition of subcontinental mantle, *Chem. Geol.*, **85**, 35–52.
- Takeuchi, T., Kodama, K. & Ozawa, T., 1999. Paleomagnetic evidence for block rotations in central Hokkaido-south Sakhalin, Northeast Asia, *Earth planet. Sci. Lett.*, **169**, 7–21.
- Tatsumoto, M., Basu, A.R., Huang, W.K., Wang, J.W. & Xie, G.H., 1992. Sr, Nd, and Pb isotopes of ultramafic xenoliths in volcanic rocks of Eastern China: enriched components EMI and EMII in subcontinental lithosphere, *Earth planet. Sci. Lett.*, **113**, 107–128.
- Uchimura, H., Kono, M., Tsunakawa, H., Kimura, G., Wei, Q., Hao, T. & Liu, H., 1996. Paleomagnetism of late Mesozoic rocks from northeastern

- China: the role of the Tan-Lu fault in the North China Block, *Tectonophysics*, **262**, 301–319.
- Uno, K., 2000. Clockwise rotation of the Korean Peninsula with respect to the North China Block inferred from an improved Early Triassic palaeomagnetic pole for the Ryeongnam Block, *Geophys. J. Int.*, **143**, 969–976.
- Uno, K. *et al.*, 1999. Late Cretaceous paleomagnetic results from North-east Asian continental margin: the Sikhote Alin mountain range, eastern Russia, *Geophys. Res. Lett.*, **26**, 553–556.
- Van der Voo, R., 1993. *Paleomagnetism of the Atlantic, Tethys and Iapetus Oceans*, p. 411, Cambridge University Press, Cambridge.
- Westphal, M., Bazhenov, M.L., Lauer, J.P., Pechersky, D.M. & Sibuet, J.-C., 1986. Paleomagnetic implications on the evolution of the Tethys belt from the Atlantic Ocean to the Pamirs since the Triassic, *Tectonophysics*, **123**, 37–82.
- Wilson, R.L., 1971. Dipole offset—the time average paleomagnetic field over the past 25 million years, *Geophys. J. R. astr. Soc.*, **22**, 491–504.
- Yang, Z.Y., Cheng, Y.Q. & Wang, H.Z., 1986. *The Geology of China*, Oxford Monographs on Geology and Geophysics, No. 3, p. 303, Clarendon Press, Oxford.
- Yokoyama, M., Liu Y.Y., Hakim, N. & Otofuji Y., 2001. Paleomagnetic study of Upper Jurassic rocks from the Sichuan basin: tectonic aspects for the collision between the Yangtze Block and the North China Block, *Earth planet. Sci. Lett.*, **193**, 273–285.
- Yukutake, T. & Tachinaka, H., 1968. The non-dipole part of the Earth's magnetic field, *Bull. Earthq. Res. Inst., Univ. Tokyo*, **46**, 1027–1074.
- Zhao, X., Coe, R.S., Gilder, S.A. & Frost, G.M., 1996. Palaeomagnetic constraints on the palaeogeography of China: implications for Gondwanaland, *Aust. J. Earth Sci.*, **43**, 643–672.
- Zhao, X.X. *et al.*, 1999. Clockwise rotations recorded in Early Cretaceous rocks of South Korea: implications for tectonic affinity between the Korean Peninsula and North China, *Geophys. J. Int.*, **139**, 447–463.
- Zijderveld, J.D.A., 1967. AC demagnetization of rocks: analysis of results, in *Methods in Paleomagnetism*, pp. 254–286, eds Collinson, D.W., Creer, K.M. & Runcorn, S.K., Elsevier, Amsterdam.
- Zonenshain, L.P., Kuzmin, M.I. & Natapov, L.M., 1990. *Geology of the USSR: a Plate-Tectonic Synthesis*, Geodyn. Ser., Vol. 21, p. 242, ed. Page, B.M., AGU, Washington, DC.